Multiple-sited interaction of caldesmon with Ca^{2+}–calmodulin

Pia A. J. HUBER*§, Mohammed EL-MEZGUELDI*, Zenon GRABAREK†, David A. SLATTER‡, Barry A. LEVINE‡ and Steven B. MARSTON*

*Imperial College, National Heart and Lung Institute, Dovehouse Street, London SW3 6LY, U.K., †Muscle Research Group, Boston Biomedical Research Institute, Boston, MA 02114, U.S.A., and ‡Department of Physiology, Medical School, University of Birmingham, Edgbaston, Birmingham B15 2TT, U.K.

The binding of Ca^{2+}– and Ba^{2+}–calmodulin to caldesmon and its functional consequence was investigated with three different calmodulin mutants. Two calmodulin mutants have pairs of cysteine residues substituted and oxidized to a disulphide bond in either the N- or C-terminal lobe (C41/75 and C85/112). The third mutant has phenylalanine-92 replaced by alanine (F92A). Binding measurements in the presence of Ca^{2+} by separation on native gels and by carbodiimide-induced cross-linking showed a lower affinity for caldesmon in all the mutants. When Ca^{2+} was replaced by Ba^{2+} the affinity of calmodulin for caldesmon was further reduced. The ability of Ca^{2+}–calmodulin to release caldesmon's inhibition of the actin–tropomyosin-activated myosin ATPase was virtually abolished by mutation of phenylalanine-92 to alanine or by replacing Ba^{2+} for Ca^{2+} in native calmodulin. Both cysteine mutants retained their functional ability, but the increased concentration needed for 50% release of caldesmon inhibition reflected their decreased affinity. Ca^{2+}–calmodulin produced a broadening in the signals of the NMR spectrum of the 10 kDa Ca^{2+}–calmodulin-binding C-terminal fragment of caldesmon arising from tryptophans −749 and −779 and caused an enhancement of maximum tryptophan fluorescence of 49% and a 16 nm blue shift of the maximum. Ca^{2+}–calmodulin F92A produced a change in wavelength of 4 nm but no change in maximum, whereas Ca^{2+}–calmodulin C41/75 binding produced a decrease in fluorescence with no shift of the maximum. We conclude that functional binding of Ca^{2+}–calmodulin to caldesmon requires multiple interaction sites on both molecules. However, some structural modification in calmodulin does not abolish the caldesmon-related functionality. This suggests that various EF hand proteins can substitute for the calmodulin molecule.

INTRODUCTION

Calmodulin belongs to the family of EF hand proteins. Two tight Ca^{2+}-binding domains, III and IV ($K_d \approx 10^{-6}$ M [1]), are located within the C-terminal lobe, which in the crystallographic structure is linked by a long solvent-exposed helix to the N-terminal lobe containing two lower affinity Ca^{2+}-specific domains, I and II ($K_d \approx 10^{-5}$ M [1]) (see review [2] and references therein). Calmodulin is able to bind to numerous, very different proteins in a Ca^{2+}-dependent manner and thus acts as a Ca^{2+} receptor and regulator of various processes within the cell. The best-described interaction of Ca^{2+}–calmodulin is the high-affinity interaction ($K_a = 10^9$ M^{-1}) with the α-helical peptide M13, which is derived from myosin light chain kinase [3,4]. Calmodulin has been shown to collapse by bending in its central helical part and to clamp its C- and N-terminal lobes around peptide M13. Similar, positively charged, amphiphilic, α-helical peptides found in several calmodulin binding proteins have been suggested to induce the same binding reaction of calmodulin [5]. However, the affinity of calmodulin for target enzymes varies, as does its conformation.

Calmodulin interacts with the smooth muscle thin-filament-associated protein, caldesmon, with an affinity in the range of 10^6 to 10^7 M^{-1}. Ca^{2+}–calmodulin is able to release caldesmon's inhibition of the actin–tropomyosin-activated myosin ATPase by forming an actin–tropomyosin–caldesmon–Ca^{2+}–calmodulin complex in which the tropomyosin is in the ON state. Three discrete sites within the C-terminus of caldesmon, A, B and B′, have been proposed for the interaction with Ca^{2+}–calmodulin (Figure 1) [6–8], and these sites flank the actin–tropomyosin binding sites, which are probably involved in inhibition. The sites in human caldesmon include or are near the tryptophan residues 716, 749 and 779 (659, 692 and 722 in chicken). An effect of Ca^{2+}–calmodulin on the tryptophan fluorescence was first shown by Shirinsky et al. [9], and we present here NMR data showing the distinct Ca^{2+}–calmodulin interaction with the two tryptophan residues 749 and 779.

Fluorescence resonance energy transfer measurements show that calmodulin binds to caldesmon in an extended conformation, different from the collapsed structure of calmodulin in the high-affinity complex with myosin light chain kinase, but similar to the troponin-C–troponin-I complex [10–12]. Since the stoichiometry is one Ca^{2+}–calmodulin per caldesmon, the extended structure introduces the possibility of different parts of calmodulin interacting with the three sites in caldesmon [9,13,14].

In order to investigate this interaction we have compared native calmodulin complexed with the unusual cation Ba^{2+} and Ca^{2+}–calmodulin mutants with native Ca^{2+}–calmodulin in the interaction with caldesmon. Ba^{2+} has an affinity of $K_a \approx 10^5$ M^{-1} to calmodulin. NMR experiments have shown a very dissimilar Ba^{2+}-induced conformational transformation of calmodulin compared with the transformation induced by Ca^{2+}. The NMR data suggest preferential binding of Ba^{2+} in the C-terminal sites III and IV of calmodulin [14a]. This predominant effect on the C-terminal lobe of calmodulin was used in addition to C-terminal

Abbreviations used: myosin-S1, myosin subfragment-1; F92A, mutant of human liver calmodulin with Ala substituted for Phe-92; C41/75, mutant of human liver calmodulin with Cys substituted for Gln-41 and Lys-75; C85/112, mutant of human liver calmodulin with Cys substituted for Ile-85 and Leu-112; DTT, 1,4-dithio-D,L-threitol.

§ To whom correspondence should be addressed.

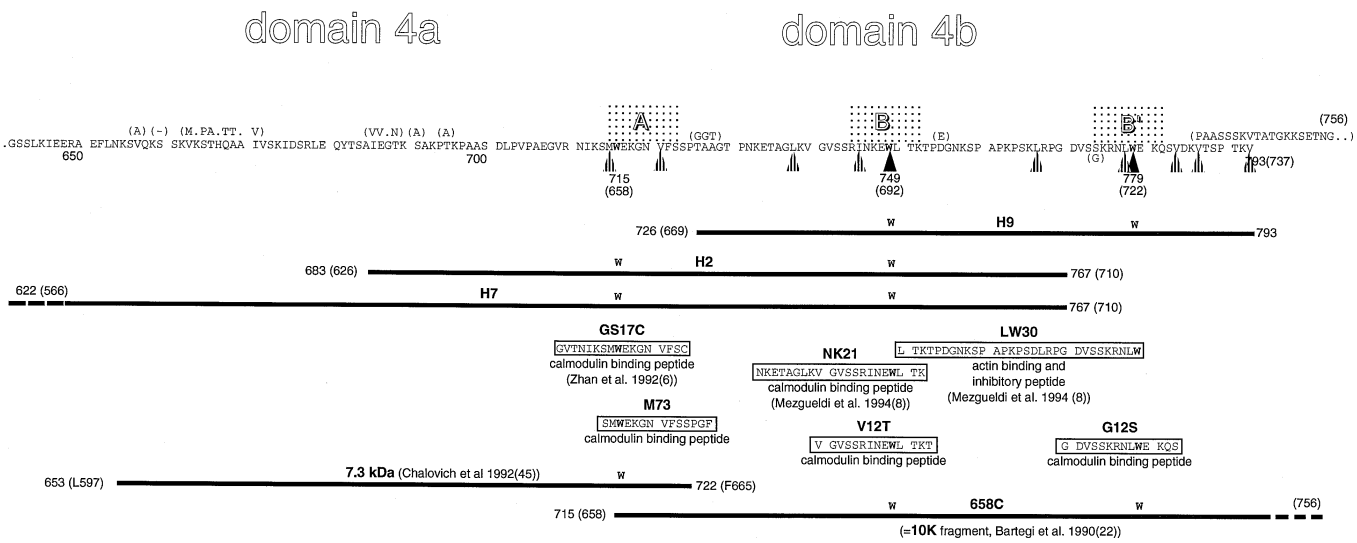

Figure 1 Amino acid sequence and calmodulin-binding sites in domain 4 of human caldesmon

The amino acid numbering is shown for human caldesmon [28] with that of chicken caldesmon [29] in brackets. The human recombinant fragments of caldesmon, H2, H7 and H9 [7], the recombinant fragment of chicken caldesmon, 658C [26], and the 7.3 kDa chymotryptic caldesmon fragment of chicken gizzard [43] are shown as black lines. The amino acid sequence of peptides M73 [7], GS17C [6], G12S, V12T [46], LW30 and NK21 [8] are shown in boxes. Arrow heads point to residues strongly (black) and slightly (hatched) affected by calmodulin SL143 in NMR experiments (see Figure 5). Calmodulin binding sites A, B and B′ are indicated as dotted rectangles.

mutant calmodulins (C85/112 and F92A) to study the effect of various perturbations in the C-terminal part of calmodulin on its ability to interact with caldesmon. The mutant C85/112 has point mutations where cysteine residues are introduced at positions 85 and 112. Oxidation of the mutant produces a stable disulphide bond within the C-terminal lobe that maintains it in the closed (Ca^{2+}-free) conformation and weakens the Ca^{2+} affinity to $\approx 1/10$ compared with native calmodulin [15]. The other C-terminal calmodulin mutant, F92A, has phenylalanine replaced with alanine at position 92, immediately preceding the first Ca^{2+} ligand, aspartic acid-93, in site III. The affinity of this mutant for Ca^{2+} is 2-fold greater than that of native calmodulin [16, 17]. Calmodulin mutant C85/112 is not able to activate phosphodiesterase or calcineurin. The mutant F92A activates phosphodiesterase to only 20%. In order to look at the effects of modifications in the N-terminal domain of calmodulin we have used the calmodulin mutant C41/75, which is the counterpart of calmodulin mutant C85/112 with a disulphide bridge between introduced cysteines at positions 41 and 75. Like its counterpart, calmodulin mutant 85/112, it has a decreased Ca^{2+} affinity and is unable to activate phosphodiesterase or calcineurin [15].

Binding, functional and tryptophan fluorescence measurements indicate that both lobes of calmodulin are involved in the interaction with caldesmon, and a two-dimensional model of the Ca^{2+}–calmodulin–caldesmon complex is deduced.

MATERIALS AND METHODS

Proteins

Native calmodulin was prepared from bovine brain according to the method of Gopalakrishna and Anderson [18]. Skeletal muscle myosin subfragment-1 (myosin-S1) and actin were prepared by standard methods [19,20]. Caldesmon was extracted from sheep aorta or from chicken gizzard by the procedures described by Taggart and Marston [21] or by Bartegi et al. [22]. Tropomyosin was prepared from sheep aorta ether ethanol powder as described by Eisenberg and Kielley [23].

The three mutant calmodulins were produced using human liver cDNA [24]. The cysteine mutations were introduced as described by Tan et al. [15]. A similar technique was used for the calmodulin mutant F92A [17] except that the mutation was introduced with the PCR technique as described by Higuchi et al. [25].

The disulphide cross-link is very stable. We have analysed the calmodulin mutants before and after exposure to 1,4-dithio-D,L-threitol (DTT) or β-mercaptoethanol, in conditions described below, by native gel analysis and did not find any alteration of the migration, indicating no change in their state of oxidization.

The caldesmon mutants 658C, H2, H7 and H9 were obtained by bacterial expression in the pMW172 plasmid /BL21(DE3) cell system described by Redwood and Marston [26] and Huber et al. [27]. Amino acid sequence numbering follows the human caldesmon sequence determination by Humphrey et al. [28]; chicken gizzard caldesmon numbers according to Bryan et al. [29] are mentioned in brackets. Protein concentrations were determined by the method of Lowry [29a].

ATPase assays

The proteins were dialysed into 5 mM Pipes (adjusted to pH 7.1 with KOH solution at 22 °C)/2.5 mM $MgCl_2$/60 mM KCl/0.1 mM DTT/(0.1 mM $CaCl_2$ or 0.28 mM $BaCl_2$ or 2.0 mM EGTA). The reaction was started in a volume of 100 μl at 37 °C by adding MgATP to 5 mM and was terminated after 10 min with 0.5 ml of 10% trichloroacetic acid. The P_i release was assayed as previously described [30].

NMR experiments

One- and two-dimensional proton NMR spectra were obtained at 500 MHz on a Bruker AMX spectrometer using quadrature detection at a sample temperature of 25 °C in ^2H_2O solution. A calmodulin species with a point mutation introducing cysteine at

position 143 was produced by Dr. C.-L. A. Wang (Boston Biomedical Research Institute, Boston, MA, U.S.A.). It was labelled with *N*-[4-(iodoacetyl)amino]-2,2,6,6-tetramethylpiperidine-1-oxyl (TEMPO-IA) spin label according to the procedure described by Gao et al. [31]. The binding titrations were carried out by addition of small aliquots of a concentrated stock solution of spin-labelled calmodulin in order to keep dilution effects below 5%.

Binding of calmodulin to caldesmon

Co-sedimentation

Direct binding was measured by co-sedimentation of caldesmon fragments, H2, H7, H9 or 658C, with native calmodulin coupled to Sepharose (Pharmacia). The protein mixtures were incubated in 5 mM Pipes (adjusted to pH 7.2 with KOH solution at 22 °C)/5 mM $MgCl_2$/30 mM KCl/0.5 mM DTT/(0.7 mM $CaCl_2$/0.5 mM EGTA or 0.7 mM $BaCl_2$/0.5 mM EGTA or 0.5 mM EGTA) in a total volume of 100 μl for 30 min at 22 °C and then centrifuged at 15000 ***g*** for 10 min. A 25 μl sample was taken before and after spinning, and the proteins were separated by gel electrophoresis on 8–18% ExcelGels (Pharmacia), run for 80 min at 10 °C, and stained with PAGE Blue 83 (Merck). The bands were quantified by densitometry (Scanmaster; Howtek; 'pdi Quantity one' software) [7].

Native gel analysis

Gels (10% polyacrylamide) ('Clean gels'; Pharmacia) in 80 mM Tris/80 mM glycine (pH 8.6)/(1 mM $CaCl_2$ and/or 0.5 mM EGTA) were used for protein separation according to Skripnikova and Gusev [32]. The proteins were loaded, and electrophoresis was at 400 V for 50 min at 10 °C. The gel was stained as described above.

Cross-linking assay

Caldesmon was cross-linked to calmodulin or calmodulin mutants as described by Grabarek and Gergely [33]. Briefly, 50 μM calmodulin or calmodulin mutant was activated for 10 min at 25 °C with 2 mM 1-ethyl-3-[3-(dimethylamino)propyl] carbodiimide in the presence of 5 mM *N*-hydroxysuccinimide in 5 mM Pipes (adjusted to pH 7.1 with KOH solution at 25 °C)/2.5 mM $MgCl_2$/10 mM KCl/0.1 mM DTT/0.2 mM $CaCl_2$. The activation was terminated by the addition of 3 mM β-mercaptoethanol, and then 10 μM caldesmon was added to a total volume of 100 μl. For cross-linking in the presence of EGTA, Ca^{2+} was omitted during the initial activation step, and the chelator (EGTA) was introduced at 2 mM into the protein solution just before the addition of caldesmon. After a 20 min incubation an aliquot of 10 μl was analysed by 8–18% SDS/PAGE as described above.

Fluorescence measurements

Fluorescence spectra were recorded on a Perkin Elmer luminescence spectrometer (LS-5) with excitation at 295 nm in 50 mM NaCl/10 mM Tris/HCl (pH 7.3)/2.5 mM $MgCl_2$/(0.1 mM $CaCl_2$ or 0.2 mM $BaCl_2$) [7,9]. Tryptophan fluorescence emission spectra (315–380 nm) were obtained from caldesmon fragments 658C, H2, H7 and H9. Calmodulin and calmodulin mutants were added from a highly concentrated stock (maximum dilution 10%). The wavelength and magnitude of maximum emission were determined from the spectra and expressed as a percentage or fractional change of the fluorescence intensity at the maximum as compared with caldesmon or caldesmon fragment alone. The reversibility of the effect was tested by the addition of EGTA at each concentration.

RESULTS

Effect of mutation in calmodulin on its reversal of the caldesmon-induced ATPase inhibition

The three calmodulin mutants, F92A, C85/112 and C41/75, and native calmodulin with the cation Ba^{2+} were tested for their ability to reverse the caldesmon-induced inhibition of the actin–tropomyosin activation of myosin MgATPase. The results are presented in Figure 2. Native Ca^{2+}–calmodulin fully reversed the inhibition, reaching 50% reversal at 8 μM. No reversal was observed in the presence of 2 mM EGTA, and only 18% reversal was found in the presence of 0.28 mM Ba^{2+}. In the presence of Ca^{2+} the two cysteine calmodulin mutants, C41/75 and C85/112, were less effective at reversing caldesmon inhibition than was native calmodulin. The N-terminal mutant, Ca^{2+}–calmodulin C41/75, reached 50% reversal at 18 μM, i.e. at 2–3-fold higher concentration when compared with native calmodulin. This mutant also showed a 30% ATPase inhibition reversal in the absence of Ca^{2+}. The C-terminal mutant, Ca^{2+}–calmodulin C85/112, was able to reverse the caldesmon inhibition to the same extent as native Ca^{2+}–calmodulin and Ca^{2+}–calmodulin C41/75; however, the amount of this mutant required was 4–5-fold higher than that of native calmodulin. In contrast the calmodulin mutant F92A showed little reversing potency of the ATPase inhibition, only 30%; moreover this slight reversal seemed to be independent of calcium ions.

Mutation in the C-terminal domain (F92A and C85/112) and the predominant effect of Ba^{2+} on the C-terminal calmodulin domain appear to be more damaging to the ability of calmodulin to reverse the caldesmon-induced inhibition of acto-myosin-S1 ATPase than mutation in the N-terminal calmodulin domain. These results suggest that the C-terminal domain of calmodulin

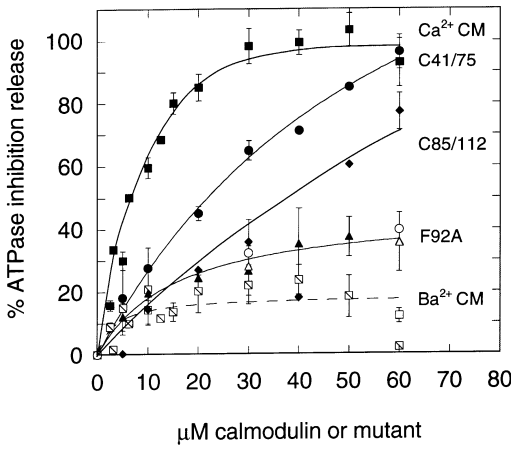

Figure 2 Reversal of the ATPase inhibition by calmodulin

The ATPase assay was carried out with 1 μM skeletal muscle myosin-S1, 10 μM skeletal muscle actin, 4 μM smooth muscle tropomyosin, 2.5 μM caldesmon and 0–60 μM calmodulin (CM) or calmodulin mutant in the presence of 0.1 mM $CaCl_2$ (closed symbols), 0.28 mM $BaCl_2$ (□) or 2 mM EGTA (open symbols) as described in the Materials and methods section. The reversal by calmodulin was expressed as a percentage of release of inhibition. Uninhibited ATPase was 1.8 s^{-1} (= 100% ATPase); inhibited ATPase was 0.6 s^{-1} (= 0% ATPase). Error bars indicated are standard errors of 2–5 experiments. Smooth curves were drawn through the data points.

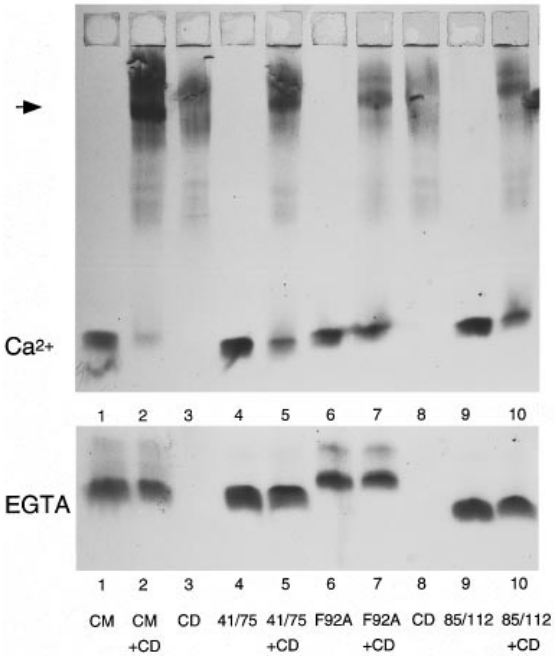

Figure 3 Co-electrophoresis of caldesmon and calmodulin or calmodulin mutants on native polyacrylamide gels

A 4.5 μg sample of calmodulin (CM) or calmodulin mutant was mixed with 24 μg of caldesmon (CD) in 5 mM Pipes (adjusted to pH 7.1 with KOH solution at 25 °C)/2.5 mM $MgCl_2$/10 mM KCl/0.1 mM DTT/(0.7 mM $CaCl_2$/0.5 mM EGTA or 0.5 mM EGTA), and the mixture was loaded on to a native polyacrylamide gel in 80 mM Tris/80 mM glycine (pH 8.6)/(1 mM $CaCl_2$/0.5 mM EGTA or 0.5 mM EGTA). The whole gel is shown for the electrophoresis in the presence of Ca^{2+}. Only the region of the calmodulin band is presented for the electrophoresis in the presence of EGTA. The arrow indicates the band of the caldesmon–calmodulin complex.

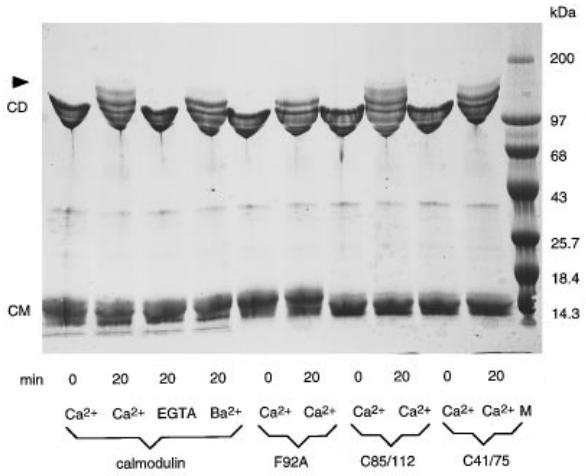

Figure 4 SDS/PAGE of caldesmon and calmodulin or calmodulin mutants after cross-linking

Aliquots of 50 μM calmodulin or calmodulin mutant (CM) and 10 μM caldesmon (CD) were used in the cross-linking reaction, which was performed with 1-ethyl-3-[3-(dimethylamino)propyl] carbodiimide/*N*-hydroxysuccinimide in 5 mM Pipes, adjusted to pH 7.1 with KOH, as described in the Materials and methods section. Samples were taken after 0 and 20 min of incubation, and the proteins were separated by SDS/PAGE as described in the Materials and methods section. M, molecular-mass markers. The arrow indicates the band of the cross-linked product (156 kDa), previously described [34].

has a predominant contribution to the activation of the caldesmon–actin–tropomyosin-myosin-S1 system by calmodulin.

Binding of calmodulin and calmodulin mutants to caldesmon

Calmodulin coupled to CNBr-activated Sepharose was used in sedimentation assays. The binding of calmodulin to caldesmon is Ca^{2+} dependent. Caldesmon fragments H2, H7, H9 and 658C (see Fig. 1 for location), co-sedimented in the presence of calcium with a binding constant in the range of 10^6 M^{-1} [7]. Hardly any co-sedimentation was found in the presence of EGTA or Ba^{2+}, indicating a binding constant of at least 20-fold lower compared with that in the presence of Ca^{2+} (results not shown).

The binding of calmodulin and calmodulin mutants to caldesmon in an equimolar mixture was tested by electrophoresis on native polyacrylamide gels at pH 8.6. Calmodulin has high mobility whereas caldesmon has very low mobility on these gels. When calmodulin is bound to caldesmon, as in the presence of Ca^{2+}, the calmodulin band is diminished and an intermediate mobility band of the caldesmon–Ca^{2+}–calmodulin complex, often quite diffuse, may be observed (Figure 3, upper panel, arrow). In the presence of EGTA no reduction of the calmodulin band was observed in the presence of caldesmon (Figure 3, lower panel). The three calmodulin mutants were found to bind to caldesmon in the presence of Ca^{2+}. However, the reduction of their bands was less than the reduction of the calmodulin band in the same assay conditions (Figure 3). With a 2-fold molar excess of caldesmon over calmodulin all the mutant calmodulin bands disappeared (results not shown); thus all the mutants can bind to caldesmon but with diminished affinity. No reduction of the band of calmodulin mutants is found in EGTA in the presence of caldesmon. The interaction of calmodulin mutants with caldesmon was studied at neutral pH using two-step zero-length cross-linking by carbodiimide. Figure 4 shows SDS/PAGE of calmodulin, calmodulin mutants and caldesmon before and after cross-linking in the presence of Ca^{2+}, EGTA or Ba^{2+}. Calmodulin can be cross-linked to caldesmon in the presence of Ca^{2+} but not in the presence of EGTA. The cross-linking product is seen as a new low-mobility band of approx. 156 kDa as described by Bartegi et al. [34]. Calmodulin was also cross-linked to caldesmon when Ca^{2+} was substituted by Ba^{2+}. Most importantly all three calmodulin mutants were also found to cross-link to caldesmon and generate the new band of low mobility, indicating again that the mutant calmodulin can bind to caldesmon. The cross-linking of the mutants to caldesmon was Ca^{2+} specific, since no cross-linked species could be observed in the presence of EGTA (results not shown).

Interaction of caldesmon–calmodulin observed by spectroscopic measurements

A Ca^{2+}–calmodulin species spin labelled at position 143 (CM SL143), was used in NMR titrations of the 99-residue C-terminal caldesmon fragment, 658C (Figure 1). This caldesmon fragment contains a mutation at position 659, where a tryptophan was replaced by glycine [26]. The ^{1}H-NMR spectrum of 658C in titration with calmodulin SL143 is shown in Figure 5. The effects observed are primarily due to the proximity of 658C residues to the paramagnetic spin label covalently linked to cysteine 143 of the calmodulin species used. Only minor signal changes are observed in the aliphatic region of the spectrum, i.e. slight broadening of the signal of methionine 715 (658) and of the overlapping signals of valine, leucine and isoleucine (Figure 5A),

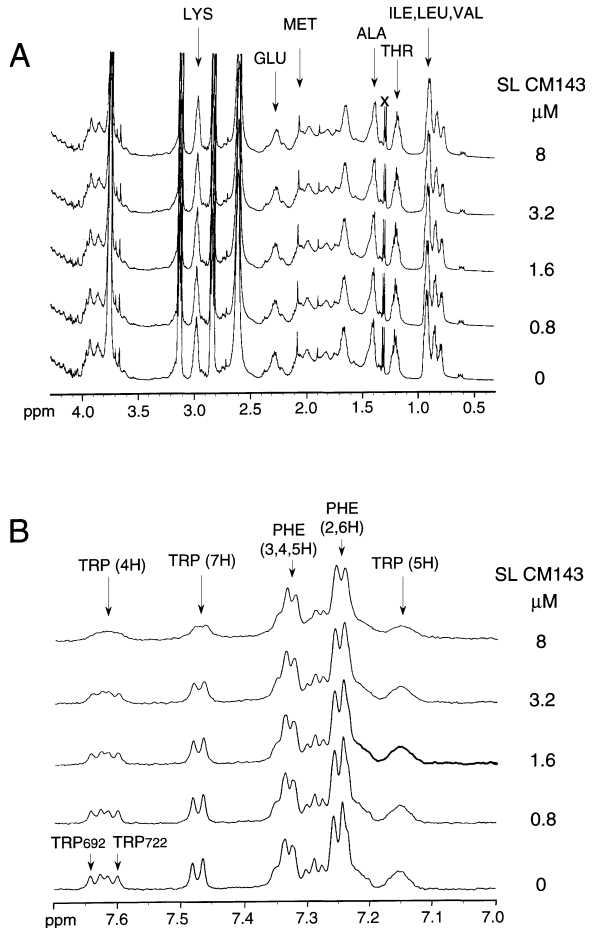

Figure 5 NMR spectra of 658C in titration with calmodulin SL143

(**A**) Aliphatic region (0.3–4.2 p.p.m.); (**B**) aromatic region (7.0–7.7 p.p.m.). Bottom trace (**A**, **B**), 400 μM 658C (caldesmon fragment); upper traces, 400 μM 658C + increasing concentrations of calmodulin SL143 (SL CM143) as indicated. Samples were made up in ^2H_2O, and the pH was adjusted by the addition of aliquots of NaO^2H or ^2HCl using direct meter readings. Chemical shifts are referenced to the internal standard 3-(trimethylsilyl)-propane sulphonic acid. (**A**) Very little change in the aliphatic region of the 658C spectrum is observed even at the highest calmodulin concentrations. (**B**) Signals at 7.15, 7.28 and 7.4–7.7 p.p.m. originating from the two tryptophan residues 749 (692) and 779 (722) are clearly broadened on titration with calmodulin SL143. The assignments of the signals at 7.64 and 7.6 are labelled in the bottom trace by arrows. (X denotes an impurity.)

whereas in the aromatic region the signals at 7.15 and 7.4–7.7 are clearly broadened on titration with Ca^{2+}–calmodulin SL143 (Figure 5B). The affected signals in the region 7.15–7.7 originate from the two tryptophan residues contained in 658C. Using two-dimensional NMR (results not shown) the signals at 7.64 and 7.6 could be further assigned to tryptophans 749 (692) and 779 (722) respectively. Both signals are affected simultaneously and equally by Ca^{2+}–calmodulin SL143.

To further characterize the interaction of caldesmon's C-terminal tryptophan residues with Ca^{2+}–calmodulin we measured the intrinsic tryptophan fluorescence of several recombinant caldesmon fragments containing different combinations of the proposed calmodulin binding sites: A (Trp-716), B (Trp-749) and B′ (Trp-779) (in the chicken sequence: 659, 692 and 722 respectively). The sequences and locations are given in Figure 1. Shirinsky et al. [9] reported that native calmodulin induces a 51 % increase of the fluorescence intensity of tryptophan and

Table 1 Changes in intrinsic tryptophan fluorescence of caldesmon fragments and peptides on titration with calmodulin and calmodulin mutants

Fluorescence spectra of caldesmon fragments 658C, H2, H7 and H9 in titrations with calmodulin or calmodulin mutants were recorded as described in the Materials and methods section. The measurements for caldesmon (CD/*h*) and the caldesmon peptides NK21 and GS17C have been included for comparison and are taken from [6,8,9].

Expressed proteins/ synthetic peptides	Sequence (human numbers)	Sequence (chicken gizzard numbers)	No. of tryptophans (positions in human sequence in brackets)	Calmodulin		Calmodulin mutant F92A		Calmodulin mutant C41/75	
				Fluorescence intensity at maximum	Shift (nm)	Fluorescence intensity at maximum	Shift (nm)	Fluorescence intensity at maximum	Shift (nm)
CD/*h*	1–793	1–756	5 (177, 417, 716, 749, 779)	↑ 51 %	351 → 339 (12 nm)	No data	No data	No data	No data
658C	715–793	658–756	2 (749, 779)	↑ 49 %	356 → 344 (16 nm)	No change	356 → 352 (4 nm)	↓ 31 %	No shift
H2	683–767	626–710	2 (716, 749)	↑ 37 %	353 → 336 (17 nm)	No change	358 → 355 (3 nm)	↓ 30 %	No shift
H7	622–767	566–710	2 (716, 749)	↑ 33 %	357 → 339 (18 nm)	No change	356 → 352 (4 nm)	No data	No data
H9	726–793	669–737	2 (749, 779)	↑ 37 %	358 → 350 (8 nm)	No change	358 → 354 (4 nm)	↓ 15 %	No shift
NK21	732–753	675–695	1 (749)	↑ 92 %	356 → 344 (12 nm)	No data	No data	No data	No data
GS17C	708–723	651–667	1 (716)	↑ 82 %	357 → 330 (27 nm)	No data	No data	No data	No data

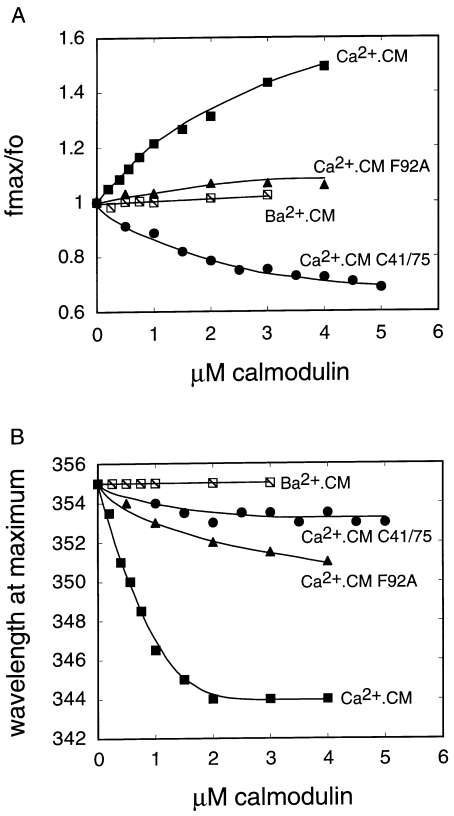

Figure 6 Effect of calmodulin and calmodulin mutants on caldesmon fragment 658C tryptophan fluorescence emission

The emission intensity (**A**) and wavelength of the maximum (**B**) of the tryptophan fluorescence of 658C were measured (excitation at 295 nm) upon titration with calmodulin (CM) or calmodulin mutants as described in the Materials and methods section. Data in (**A**) are expressed as a fractional change of the fluorescence intensity at the maximum as compared with 658C alone.

shifts the maximum from 351 to 339 nm. Similarly we have observed that the C-terminal fragments, H2 and H7 with Trp-716 and -749 (659 and 692 in the chicken sequence) and 658C and H9 with Trp-749 and -779 (692 and 722), show a fluorescence intensity increase of the spectrum maximum of 33 % to 49 % and a shift of the maximum of 8 nm to 18 nm on interaction with calmodulin. Previous fluorescence intensity measurements for the interaction of caldesmon with calmodulin were performed at a fixed wavelength (320 nm) [7,9,14,35]. However, the intensities measured at 320 nm are the function of the fluorescence intensity change and the blue shift. We have measured the fluorescence intensities at the spectrum maximum, wherever this shifted to. Results of the titrations are presented in Table 1. Figure 6 illustrates the fluorescence changes due to calmodulin observed with the caldesmon 658C fragment, which contains two Trp residues at positions 749 (692) and 779 (722). 658C was titrated with native calmodulin in the presence of Ca^{2+} or Ba^{2+} and with the calmodulin mutants C41/75 and F92A. The intensity increase and maximum shift are not observed in the presence of Ba^{2+}–calmodulin. Mutation within the C-terminal lobe of calmodulin (F92A) results in no fluorescence intensity change; however, a small shift of the wavelength maximum of 4 nm was observed. The N-terminal calmodulin mutant C41/75 caused a considerable decrease of the Trp fluorescence intensity, but no shift of the fluorescence maximum was induced. The reactions with the calmodulin mutants were only partially reversible in EGTA. The other caldesmon fragments, H2, H7 and H9, reacted very similarly to the caldesmon fragment 658C. The results are summarized in Table 1, which also includes fluorescence data of two peptides, GS17C and NK21 (taken from [6] and [8]), for comparison.

DISCUSSION

Ca^{2+}–calmodulin binds to caldesmon and reverses the caldesmon inhibition of the actin–tropomyosin-activated myosin MgATPase. Previous work has identified three interaction sites in the C-terminus of caldesmon, but the location of corresponding sites in calmodulin is unknown. We have tested the interaction of calmodulin with caldesmon in NMR experiments by fluorescence measurements, native gel analysis, chemical cross-linking and functional assays.

NMR of the C-terminal caldesmon fragment 658C showed a clear effect of the spin-label probe at cysteine 143 of Ca^{2+}–calmodulin on the C-terminal tryptophan residues 749 (692) and 779 (722). The effect on these tryptophans seems to be separate from the first-characterized binding site A, which has been located around tryptophan-716, and indicates interaction of calmodulin with several distinct sites on caldesmon, in agreement with previous work [7]. The comparison of tryptophan fluorescence changes with different fragments of caldesmon (in Table 1) suggests that the bulk of the fluorescence change on Ca^{2+}–calmodulin binding is associated with a single tryptophan: 749 (692) in site B.

We have used the divalent cation Ba^{2+} in comparison with Ca^{2+} and EGTA and several calmodulin mutants to determine whether the multiple site effects on caldesmon are reflected on the calmodulin molecule.

Ba^{2+} has a substantially higher ionic radius (1.34 Å) than Ca^{2+} (0.99 Å). It has been suggested that Ba^{2+} binds preferentially to the C-terminal sites III and IV in calmodulin [14a]. In fact we found that the substitution of Ba^{2+} for Ca^{2+} decreased the binding of calmodulin to caldesmon and totally abolished its functional potency. A mutation within the C-terminal lobe of calmodulin, where phenylalanine-92 is replaced by alanine (F92A), induced a similar behaviour to that induced by the replacement of Ca^{2+} by Ba^{2+}. Binding of Ca^{2+}–calmodulin F92A to caldesmon was reduced, and it had only a very minor and Ca^{2+}-independent releasing effect on the caldesmon inhibition of the actin–tropomyosin-activated myosin MgATPase activity. The mutation F92A results in a 2-fold increase in Ca^{2+} affinity [16,17]; however, the inability of this mutant to reverse the ATPase inhibition at higher concentrations where it most probably binds, based on the results from native gel and cross-linking measurements, indicates a significant conformational change caused by the mutation which is reflected in the greatly reduced changes observed in tryptophan fluorescence titrations. It is plausible that the functional consequence of the F92A mutation results from a change in the conformation or accessibility of side chains of methionines and other hydrophobic residues in the C-terminal domain of calmodulin. Methionine residues have been implicated in hydrophobic interactions of calmodulin owing to their conformational flexibility and an overall large contribution (46 %) to the accessible surface area of the molecule [5]. Phenylalanine-92 and methionines -109, -124,-144 and -145 are involved in the C-terminal hydrophobic cleft of calmodulin [36].

Two calmodulin mutants, C41/75 and C85/112, with N- or C-terminal lobes constrained in a Ca^{2+}-free conformation were surprisingly able to release to a large extent the caldesmon inhibition of the actin–tropomyosin-activated myosin

MgATPase, although they are unable to activate phosphodiesterase and calcineurin [15]. It is therefore not essential for the interaction with caldesmon that the Ca^{2+}-induced conformational change, typical of the native molecule, happens simultaneously in both lobes of calmodulin; in fact one domain (the C-terminal one in particular) may be sufficient for all or most of the activation. Accordingly binding measurements showed that these 'disulphide-fixed' calmodulin mutants bound to caldesmon, although with lower affinity. In tryptophan fluorescence titrations with caldesmon fragments Ca^{2+}–calmodulin C41/75 caused a decrease of the fluorescence maximum, indicating that the binding-induced conformation of caldesmon fragments is significantly different from the one induced by native calmodulin. The tryptophans of caldesmon do not move into a hydrophobic environment upon binding to Ca^{2+}–calmodulin mutant C41/75 as they do upon binding to native Ca^{2+}–calmodulin; thus tryptophan fluorescence increase and blue shift do not correlate with functional effects. Different positioning of methionine side chains in the mutant may be the cause of this result, as three methionines, 71, 72 and 76, are close to the disulphide bond of C41/75. Medvedeva et al. [35] also observed altered calmodulin-induced changes in the fluorescence spectra of caldesmon for two N-terminal calmodulin mutants with alteration of the first or of the second Ca^{2+}-binding loop of calmodulin.

Calmodulin interacts with its targets in a very flexible manner. Short peptides with repeats of hydrophobic and positively charged residues, such as for example M13, the calmodulin-binding peptide of myosin light chain kinase, have been observed to form an α-helical structure upon binding to calmodulin. Calmodulin has been found to clamp around these so-called BAA motifs (basic, amphiphilic and α-helices) [5]. Indeed a corresponding interaction of the caldesmon peptide GS17C with calmodulin has been observed by NMR [37]. However, the behaviour of isolated peptides may not always reflect the behaviour of the same sequence within the parent protein. This is likely to be true for caldesmon, since fluorescence resonance energy transfer measurements show that Ca^{2+}–calmodulin has an extended conformation in a complex with intact caldesmon but not in complexes with short synthetic peptides corresponding to calmodulin-binding sites of caldesmon [10]. Thus the caldesmon–calmodulin interaction resembles the troponin-I–troponin-C interaction structurally [11,12,38] rather than the myosin light chain kinase–calmodulin interaction; this is an attractive analogy, since extensive work shows that the caldesmon–actin–tropomyosin interaction closely resembles the troponin–actin–tropomyosin interaction [39,40].

Based on our observations of caldesmon fragments and calmodulin mutants we propose a model of interaction depicted in Figure 7. Graceffa and Jancso [41] have shown that the C-terminus of caldesmon has hardly any secondary structure, and Mornet et al. [42] have proposed that it may take up a looped or spiralled conformation, accounting for the measured proximity of cysteine-636 (580) to tyrosine-682 (625), histidine-667 (610) and tryptophans -716, -749 and -779 (659, 692 and 722). Ca^{2+}–calmodulin interacts with several sites within this structure simultaneously, positioning its hydrophobic residues near the tryptophan residues of the caldesmon molecule and stabilizing the folded structure. Alternatively, at partial saturation, Ca^{2+}–calmodulin may (C-terminally) anchor at one point on caldesmon (site B) and wobble between other sites with its second lobe. Such an interaction accounts for the effects of calmodulin on caldesmon observed in NMR spectra where [caldesmon] $\gg$ [calmodulin] (Figure 5). This type of interaction has been described for troponin-C–troponin-I by Dalgarno et al. [11]. In addition Olah and Trewhella [38] have proposed a model

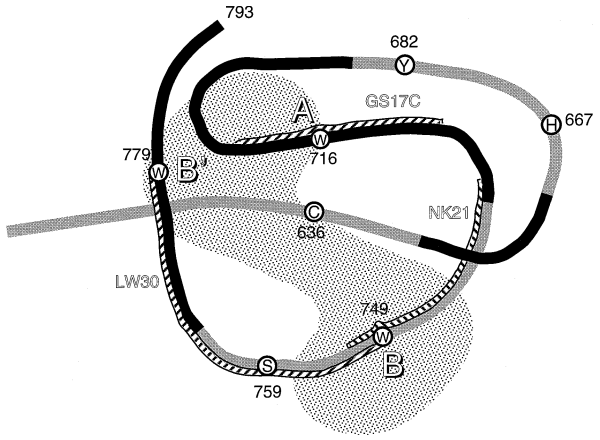

Figure 7 Model of the two-dimensional structure of domain 4 derived from structural and functional studies [42]

This hypothetical structure shows domain 4 of caldesmon bound to Ca^{2+}–calmodulin. Sites A, B and B′ are indicated as including both lobes of calmodulin bound in an extended conformation, together with caldesmon tryptophans -716, -749 and -779. The peptide chain is looped so that the three tryptophans, histidine-667 and tyrosine-682 are within 1.5 nm of cysteine-636 [42]; see Marston and Huber [39] for a rationale of this model. The exons are indicated by alternating shading of the peptide chain. Exon 11 is the loop at the bottom, which includes tryptophan-749 and the MAP kinase site, serine-759.

structure derived from small-angle X-ray and neutron-scattering data where troponin-I appears as a spiral structure that wraps around the dumbbell configuration of $(Ca^{2+})_4$–troponin-C. This structure is similar to our proposed model in Figure 7. The importance of multiple point binding as a stabilizing factor is supported by competition experiments in which H2 and the peptide NK21 reverse calmodulin's functional effect by displacing calmodulin from one {site B by NK21(results not shown) or site A by GS17C [43]} or two (sites A and B by H2 [7]) of the three putative sites.

We conclude that calmodulin seems to be able to bind functionally to caldesmon in more than one particular manner. An essential feature is, however, the involvement of multiple (two or three) sites on caldesmon and on calmodulin for functional interaction. Both domains of calmodulin are involved in the interaction with caldesmon, and the C-terminal lobe seems to contribute predominantly to the activation of the caldesmon–acto-myosin-S1 system by calmodulin. Site B on caldesmon is essential for the coupling of calmodulin binding to neutralization of the actin–tropomyosin-activated myosin ATPase inhibition, whereas sites A and B′ may substitute for one another in shorter caldesmon fragments. This multiple site interaction results in a certain fixation of the C-terminal domain 4 of caldesmon, as modelled schematically in Figure 7, but provides a versatile model for regulation. Fixing caldesmon in complex with Ca^{2+}–calmodulin would prevent caldesmon achieving the conformation and the contacts to actin required for its inhibitory function. The 'fixing' points may vary to a certain extent, allowing for variations in the Ca^{2+}-binding protein as demonstrated by the cysteine calmodulin mutants C41/75 and C85/112. This 'flexible' and, perhaps, not very specific type of interaction may explain why calmodulin is not the only EF hand protein able to reverse the caldesmon inhibition. Troponin-C, caltropin or S100, the latter most probably interacting as a dimer, can interact with caldesmon and release inhibition [13,32,44].

We thank Yasuko Mabuchi for her excellent technical assistance in the production of the calmodulin mutants and Iain Fraser for the production of the caldesmon fragments H7 and H9. This work was supported by the British Heart Foundation and by the National Institutes of Health (grants AR-41156 and P01AR-41637).

REFERENCES

1 Linse, S., Helmersson, A. and Forsen, S. (1991) J. Biol. Chem. **266**, 8050–8054
2 Weinstein, J. and Mehler, E. L. (1994) Annu. Rev. Physiol. **56**, 213–236
3 Ikura, G., Clore, G. M., Gronenborn, A. M., Zhu, G., Klee, C. B. and Bax, A. (1992) Science **256**, 632–638
4 Meador, W. E., Means, A. R. and Quiocho, F. A. (1992) Science **257**, 1251–1255
5 O'Neil, K. T. and DeGrado, W. F. (1990) Trends Biochem. Sci. **15**, 59–64
6 Zhan, Q., Wong, S. S. and Wang, C.-L. A. (1991) J. Biol. Chem. **266**, 21810–21814
7 Marston, S. B., Fraser, I. D. C., Huber, P. A. J., Pritchard, K., Gusev, N. B. and Torok, K. (1994) J. Biol. Chem. **269**, 8134–8139
8 Mezgueldi, M., Derancourt, J., Callas, B., Kassab, R. and Fattoum, A. (1994) J. Biol. Chem. **269**, 12824–12832
9 Shirinsky, V. P., Bushueva, T. L. and Frolova, S. I. (1988) Biochem. J. **255**, 203–208
10 Mabuchi, Y., Wang, C.-L. A. and Grabarek, Z. (1995) Biophys. J. **68**, A359
11 Dalgarno, D. C., Grand, R. J. A., Levine, B. A., Moir, A. J. G., Scott, G. M. M. and Perry, S. V. (1982) FEBS Lett. **150**, 54–58
12 Gong, B.-J., Wang, Z., Tao, T. and Gergely, J. (1994) Biophys. J. **66**, A346
13 Pritchard, K. and Marston, S. B. (1989) Biochem. J. **257**, 839–843
14 Malencik, D. A., Ausio, J., Byles, C. E., Modrell, B. and Anderson, S. R. (1989) Biochemistry **28**, 8227–8233
14a Klevit, R. K. (1981) Ph.D. Thesis, Oxford University
15 Tan, R.-Y., Mabuchi, Y. and Grabarek, Z. (1996) J. Biol. Chem. **271**, 7479–7483
16 Meyer, D. F. and Grabarek, Z. (1995) Biophys. J. **68**, A164
17 Meyer, D. F., Mabuchi, Y. and Grabarek, Z. (1996) J. Biol. Chem., in the press
18 Gopalakrishna, R. and Anderson, W. B. (1982) Biochem. Biophys. Res. Commun. **104**, 830–836
19 Margossian, S. S. and Lowey, S. (1982) Methods Enzymol. **85**, 55–71
20 Straub, F. B. (1942) Studies from the Institute of Medical Chemistry, University of Szeged **2**, 3–16
21 Taggart, M. J. and Marston, S. B. (1988) FEBS Lett. **242**, 171–174
22 Bartegi, A., Fattoum, A. and Kassab, R. (1990) J. Biol. Chem. **265**, 2231–2237
23 Eisenberg, E. and Kielley, W. W. (1974) J. Biol. Chem. **249**, 4742–4748
24 Wawrzynczak, E. J. and Perham, R. N. (1984) Biochem. Internat. **9**, 177–185
25 Higuchi, R., Krummel, B. and Saiki, R. K. (1988) Nucleic Acids Res. **16**, 7351–7367
26 Redwood, C. S. and Marston, S. B. (1993) J. Biol. Chem. **268**, 10969–10976
27 Huber, P. A. J., Fraser, I. D. C. and Marston, S. B. (1995) Biochem. J. **312**, 617–625
28 Humphrey, M. B., Herrera-Sosa, H., Gonzalez, G., Lee, R. and Bryan, J. (1992) Gene **112**, 197–205
29 Bryan, J., Imai, M., Lee, R., Moore, P., Cook, R. G. and Lin, W. G. (1989) J. Biol. Chem. **264**, 13873–13879
29a Lowry, O. H., Rosebrough, N. J., Farr, A. L. and Randall, R. J. (1951) J. Biol. Chem. **193**, 265–275
30 Smith, C. W., Pritchard, K. and Marston, S. B. (1987) J. Biol. Chem. **262**, 116–122
31 Gao, Y., Levine, B. A., Mornet, D., Slatter, D. A. and Strasburg, G. M. (1992) Biochim. Biophys. Acta **1160**, 22–34
32 Skripnikova, E. V. and Gusev, N. B. (1989) FEBS Lett. **257**, 380–382
33 Grabarek, Z. and Gergely, J. (1990) Anal. Biochem. **185**, 131–135
34 Bartegi, A., Fattoum, A., Derancourt, J. and Kassab, R. (1990) J. Biol. Chem. **265**, 15231–15238
35 Medvedeva, M. V., Bushueva, T. L., Shirinsky, V. P., Lukas, T. J., Watterson, D. M. and Gusev, N. B. (1995) FEBS Lett. **360**, 89–92
36 Babu, Y. S., Bugg, C. E. and Cook, W. J. (1988) J. Mol. Biol. **204**, 191–204
37 Zhang, M. and Vogel, H. J. (1994) Biochemistry **33**, 1163–1171
38 Olah, G. A. and Trewhella, J. (1994) Biochemistry **33**, 12800–12806
39 Marston, S. B. and Huber, P. A. J. (1996) in Biochemistry of Smooth Muscle Contraction (Barany, M. and Barany, K., eds.), pp. 77–90, Academic Press, New York, London, Sydney and Tokyo
40 Marston, S. B., Fraser, I. D. C. and Huber, P. A. J. (1994) J. Biol. Chem. **269**, 32104–32109
41 Graceffa, P. and Jancso, A. (1993) Arch. Biochem. Biophys. **307**, 21–28
42 Mornet, D., Bonet-Kerrache, A., Strasburg, G. M., Patchell, V. B., Perry, S. V., Huber, P. A. J., Marston, S. B., Slatter, D. A., Evans, J. S. and Levine, B. A. (1995) Biochemistry **34**, 1893–1901
43 Zhuang, S., Wang, E. and Wang, C.-L. A. (1995) J. Biol. Chem. **270**, 19964–19968
44 Mani, R. S., McCubbin, W. D. and Kay, C. M. (1992) Biochemistry **31**, 11896–11901
45 Chalovich, J. M., Bryan, J., Benson, C. E. and Velaz, L. (1992) J. Biol. Chem. **267**, 16644–16650
46 Huber, P. A. J., Grabarek, Z., Slatter, D. A., Levine, B. A. and Marston, S. B. (1995) Biophys. J. **68**, A59

Received 20 December 1995; accepted 26 January 1996